Selective patterned growth of ZnO nanowires/nanosheets and their photoluminescence properties

Kai Chen,[1,2,4] Dao D. Thang,[1,2,3] Satoshi Ishii,[1,2] Ramu P. Sugavaneshwa,[1,2] and Tadaaki Nagao[1,2*]

[1] *International Center for Materials Nanoarchitectonics (MANA), National Institute for Materials Science (NIMS), 1-1 Namiki, Tsukuba, Ibaraki 305-0044, Japan*

[2] *CREST, Japan Science and Technology Agency, 4-1-8 Honcho, Kawaguchi, Saitana, 332-0012, Japan*
[3] *Graduate School of Materials Science, Nara Institute of Science and Technology, Japan*
[4]*Chen.Kai@nims.go.jp*
**Nagao.Tadaaki@nims.go.jp*

Abstract: Zinc oxide (ZnO) demonstrates promising applications in photocatalysis, photodetectors and light-emitting devices. The shape of the ZnO nanoparticles plays an important role in determining their mechanical and optical properties. Here we report facile and controllable synthesis of ZnO nanowires and nanosheets with hydrothermal synthesis on patterned aluminum substrates prepared by colloidal lithography. The nanowire areas and nanosheet areas were well-defined in micron scale and they displayed dramatically different photoluminescence properties: while nanowires showed strong band-edge emission at 382 nm with a moderate orange emission at 600 nm, nanosheets only showed broad and intense green emission in the 547 nm range. The method demonstrated here enables periodic ZnO nanowire/nanosheet patterning with well-controlled morphology and luminescence property, which would provide a large-scale facile fabrication technique to tailor the substrate's optical properties by using ZnO as the only constituent oxide component.

OCIS codes: (160.4670) Optical materials; (220.4241) Nanostructure fabrication; (250.5230) Photoluminescence.

References and links

1. T. D. Dao, C. T. T. Dang, G. Han, C. V. Hoang, W. Yi, V. Narayanamurti, and T. Nagao, "Chemically synthesized nanowire TiO2/ZnO core-shell p-n junction array for high sensitivity ultraviolet photodetector," Appl. Phys. Lett. **103**(19), 193119 (2013).
2. L. T. Singh, R. P. Sugavaneshwar, and K. K. Nanda, "Carbon nanotube-ZnO nanowire hybrid architectures as multifunctional devices," AIP Advances **3**(8), 082106 (2013).
3. S. L. Shinde and K. K. Nanda, "Wide-Range Temperature Sensing using Highly Sensitive Green-Luminescent ZnO and PMMA-ZnO Film as a Non-Contact Optical Probe," Angew. Chem. Int. Ed. Engl. **52**(43), 11325–11328 (2013).
4. J. X. Wang, X. W. Sun, Y. Yang, H. Huang, Y. C. Lee, O. K. Tan, and L. Vayssieres, "Hydrothermally grown oriented ZnO nanorod arrays for gas sensing applications," Nanotechnology **17**(19), 4995–4998 (2006).
5. M.-W. Ahn, K.-S. Park, J.-H. Heo, J.-G. Park, D.-W. Kim, K. J. Choi, J.-H. Lee, and S.-H. Hong, "Gas sensing properties of defect-controlled ZnO-nanowire gas sensor," Appl. Phys. Lett. **93**(26), 263103 (2008).
6. M. Liu, C.-Y. Nam, C. T. Black, J. Kamcev, and L. Zhang, "Enhancing Water Splitting Activity and Chemical Stability of Zinc Oxide Nanowire Photoanodes with Ultrathin Titania Shells," J. Phys. Chem. C **117**(26), 13396–13402 (2013).
7. Y. L. Chen, L.-C. Kuo, M. L. Tseng, H. M. Chen, C.-K. Chen, H. J. Huang, R.-S. Liu, and D. P. Tsai, "ZnO nanorod optical disk photocatalytic reactor for photodegradation of methyl orange," Opt. Express **21**(6), 7240–7249 (2013).
8. H. M. Chen, C. K. Chen, M. L. Tseng, P. C. Wu, C. M. Chang, L.-C. Cheng, H. W. Huang, T. S. Chan, D.-W. Huang, R.-S. Liu, and D. P. Tsai, "Plasmonic ZnO/Ag Embedded Structures as Collecting Layers for Photogenerating Electrons in Solar Hydrogen Generation Photoelectrodes," Small **9**(17), 2926–2936 (2013).

#226727 - $15.00 USD Received 12 Nov 2014; accepted 18 Dec 2014; published 13 Jan 2015

9. K.-H. Kim, B. Kumar, K. Y. Lee, H.-K. Park, J.-H. Lee, H. H. Lee, H. Jun, D. Lee, and S.-W. Kim, "Piezoelectric two-dimensional nanosheets/anionic layer heterojunction for efficient direct current power generation," Sci Rep **3**, 2017 (2013).
10. Z. L. Wang and J. Song, "Piezoelectric Nanogenerators Based on Zinc Oxide Nanowire Arrays," Science **312**(5771), 242–246 (2006).
11. C. W. Chen, S. C. Hung, C. H. Lee, C. J. Tun, C. H. Kuo, M. D. Yang, C. W. Yeh, C. H. Wu, and G. C. Chi, "Nonpolar light emitting diode made by m-plane n-ZnO/p-GaN heterostructure," Opt. Mater. Express **1**(8), 1555–1560 (2011).
12. H.-Y. Shih, S.-H. Cheng, J.-K. Lian, T.-Y. Lin, and Y.-F. Chen, "Light-emitting devices with tunable color from ZnO nanorods grown on InGaN/GaN multiple quantum wells," Opt. Express **20**(S2 Suppl 2), A270–A277 (2012).
13. L. E. Greene, M. Law, D. H. Tan, M. Montano, J. Goldberger, G. Somorjai, and P. Yang, "General Route to Vertical ZnO Nanowire Arrays Using Textured ZnO Seeds," Nano Lett. **5**(7), 1231–1236 (2005).
14. S. Xu and Z. Wang, "One-dimensional ZnO nanostructures: Solution growth and functional properties," Nano Res. **4**(11), 1013–1098 (2011).
15. N. Wang, H. Lin, J. Li, L. Zhang, X. Li, J. Wu, and C. Lin, "Strong Orange Luminescence from a Novel Hexagonal ZnO Nanosheet Film Grown on Aluminum Substrate by a Simple Wet-Chemical Approach," J. Am. Ceram. Soc. **90**(2), 635–637 (2007).
16. L. Hongjun, Z. Zang, and X. Tang, "Synthesis mechanism and optical properties of well nanoflower-shaped ZnO fabricated by a facile method," Opt. Mater. Express **4**(9), 1762–1769 (2014).
17. S. Baruah and J. Dutta, "Hydrothermal growth of ZnO nanostructures," Sci. Technol. Adv. Mater. **10**(1), 013001 (2009).
18. Y. Tong, Y. Liu, L. Dong, D. Zhao, J. Zhang, Y. Lu, D. Shen, and X. Fan, "Growth of ZnO Nanostructures with Different Morphologies by Using Hydrothermal Technique," J. Phys. Chem. B **110**(41), 20263–20267 (2006).
19. B. D. Choudhury, A. Abedin, A. Dev, R. Sanatinia, and S. Anand, "Silicon micro-structure and ZnO nanowire hierarchical assortments for light management," Opt. Mater. Express **3**(8), 1039–1048 (2013).
20. Y. H. Ko and J. S. Yu, "Design of hemi-urchin shaped ZnO nanostructures for broadband and wide-angle antireflection coatings," Opt. Express **19**(1), 297–305 (2011).
21. C. L. Haynes and R. P. Van Duyne, "Nanosphere Lithography: A Versatile Nanofabrication Tool for Studies of Size-Dependent Nanoparticle Optics," J. Phys. Chem. B **105**(24), 5599–5611 (2001).
22. K. Chen, S. V. Stoianov, J. Bangerter, and H. D. Robinson, "Restricted meniscus convective self-assembly," J. Colloid Interface Sci. **344**(2), 315–320 (2010).
23. M. C. Gwinner, E. Koroknay, L. Fu, P. Patoka, W. Kandulski, M. Giersig, and H. Giessen, "Periodic Large-Area Metallic Split-Ring Resonator Metamaterial Fabrication Based on Shadow Nanosphere Lithography," Small **5**(3), 400–406 (2009).
24. X. Wang, C. J. Summers, and Z. L. Wang, "Large-Scale Hexagonal-Patterned Growth of Aligned ZnO Nanorods for Nano-optoelectronics and Nanosensor Arrays," Nano Lett. **4**(3), 423–426 (2004).
25. D. F. Liu, Y. J. Xiang, X. C. Wu, Z. X. Zhang, L. F. Liu, L. Song, X. W. Zhao, S. D. Luo, W. J. Ma, J. Shen, W. Y. Zhou, G. Wang, C. Y. Wang, and S. S. Xie, "Periodic ZnO Nanorod Arrays Defined by Polystyrene Microsphere Self-Assembled Monolayers," Nano Lett. **6**(10), 2375–2378 (2006).
26. C. Li, G. Hong, P. Wang, D. Yu, and L. Qi, "Wet Chemical Approaches to Patterned Arrays of Well-Aligned ZnO Nanopillars Assisted by Monolayer Colloidal Crystals," Chem. Mater. **21**(5), 891–897 (2009).
27. D. Li, Y. H. Leung, A. B. Djurišić, Z. T. Liu, M. H. Xie, S. L. Shi, S. J. Xu, and W. K. Chan, "Different origins of visible luminescence in ZnO nanostructures fabricated by the chemical and evaporation methods," Appl. Phys. Lett. **85**(9), 1601–1603 (2004).
28. K. H. Tam, C. K. Cheung, Y. H. Leung, A. B. Djurisić, C. C. Ling, C. D. Beling, S. Fung, W. M. Kwok, W. K. Chan, D. L. Phillips, L. Ding, and W. K. Ge, "Defects in ZnO Nanorods Prepared by a Hydrothermal Method," J. Phys. Chem. B **110**(42), 20865–20871 (2006).
29. A. Janotti and C. G. Van de Walle, "Native point defects in ZnO," Phys. Rev. B **76**(16), 165202 (2007).
30. A. Janotti and C. G. V. Walle, "Fundamentals of zinc oxide as a semiconductor," Rep. Prog. Phys. **72**(12), 126501 (2009).
31. A. B. Djurišić, Y. H. Leung, K. H. Tam, Y. F. Hsu, L. Ding, W. K. Ge, Y. C. Zhong, K. S. Wong, W. K. Chan, H. L. Tam, K. W. Cheah, W. M. Kwok, and D. L. Phillips, "Defect emissions in ZnO nanostructures," Nanotechnology **18**(9), 095702 (2007).
32. M. Willander, O. Nur, J. R. Sadaf, M. I. Qadir, S. Zaman, A. Zainelabdin, N. Bano, and I. Hussain, "Luminescence from Zinc Oxide Nanostructures and Polymers and their Hybrid Devices," Materials **3**(4), 2643–2667 (2010).
33. F. Fabbri, M. Villani, A. Catellani, A. Calzolari, G. Cicero, D. Calestani, G. Calestani, A. Zappettini, B. Dierre, T. Sekiguchi, and G. Salviati, "Zn vacancy induced green luminescence on non-polar surfaces in ZnO nanostructures," Sci Rep **4**, 5158 (2014).

1. Introduction

ZnO is an attractive semiconductor oxide with direct band-gap of 3.3 eV and large exciton binding energy of 60 meV. Many promising applications for ZnO have been proposed as UV

#226727 - $15.00 USD Received 12 Nov 2014; accepted 18 Dec 2014; published 13 Jan 2015

photodetectors [1, 2], sensors [3–5], photocatalytic materials [6–8], piezoelectric devices [9, 10], and light-emitting devices [11, 12]. In particular, low-dimensional ZnO nanoparticles have received considerable attentions due to their large surface-to-volume ratios. The optical, electrical and mechanical properties of ZnO nanoparticles are highly dependent on their dimensionality, shape and surface morphology. A great variety of ZnO nanoparticles with different morphologies, including nanowire, nanotube and nanoplate, have been fabricated [13–16]. A large number of studies have been devoted to their optical property since it can be varied dramatically through the incorporation of surface defects which are largely affected by the crystal growth procedures. To control the crystal growth, methods like template-assisted or surfactant-mediated growth are often adopted for tuning the morphologies in physical growth methods such as molecular beam epitaxy and vapor-liquid-solid phase (VLS) growth. But few studies have been reported so far on wet chemical synthesis combined with template-assisted growth [17, 18]. In particular, hydrothermal synthesis of ZnO nanostructures has seen rising popularity in recent years as it is a low-cost and environment-friendly wet chemical technique. Combination with selective growth would give rise to big advantage for controlling the morphologies as well as tailoring the optical and mechanical properties of the ZnO nanostructures.

Besides the particle shapes, it is also of great importance to be able to fabricate large-scale periodic patterns of the ZnO nanostructures adaptable for a range of applications [19, 20]. Colloidal lithography (it is also generally referred as nanosphere lithography) [21–23], which provides outstanding control to create large-area periodic patterns, has been used to create ZnO nanorod/nanopillar array [24–26], where only one type of nanostructure was fabricated. Herein, combining hydrothermal synthesis with colloidal lithography, we demonstrate nano-patterning of periodic ZnO nanowire/nanosheet hybrid nanostructures. Al nanohole array was fabricated by colloidal lithography on indium tin oxide (ITO) substrates and subsequently ZnO nanowires grew inside the holes while nanosheets exclusively grew on the Al-covered area in the same growth solution. The nanostructures were characterized by photoluminescence (PL), energy-dispersive x-ray spectroscopy (EDS) and TEM. The method presented here can be applied in a number of applications, from widening the active spectral region of ZnO-based light-emitting devices to down-conversion for photovoltaics and photocatalyst applications.

2. Experiments

2.1 ZnO nanoparticle synthesis

The ZnO nanowire/nanosheet array was synthesized on ITO glass substrates by hydrothermal method combined with colloidal lithography as illustrated in Fig. 1. The ITO glass substrates were cleaned using acetone, ethanol and de-ionized water (5 min sonication for each cleaning step). Mixed solution of zinc acetate dihydrate [$Zn(C_2H_3O_2)_2{\cdot}2H_2O$] (0.3 M) and monoethanolamine (MEA) solution (0.3 M) in ethanol was spin-coated onto the substrates three times at 3000 rpm for 30s. A ZnO seed layer was then formed on the ITO glass substrates. The seed layer was dried at room temperature and annealed in ambient air at 300 °C for one hour.

Colloidal lithography was then performed on the substrates. Polystyrene spheres (PS) with diameter of 4.4 μm were chosen as the original lithography masks to create the patterned Al nanohole arrays (We use the term “nanohole” because the thickness of the nanohole is 50 nm even though its lateral dimension is in μm range). Firstly, a monolayer of PS spheres was prepared on top of the ZnO seeds/ITO glass substrates. To shrink the PS spheres, reactive ion etching (RIE) was employed using O_2 gas with an etching rate of 3.1 nm/second. The designed lithography masks with different sizes were obtained by controlling the etching time. Then an Al film of 50 nm was deposited onto the substrates using electron beam

#226727 - $15.00 USD Received 12 Nov 2014; accepted 18 Dec 2014; published 13 Jan 2015

deposition. The patterned ZnO seed layer was finally achieved by removing the etched PS arrays.

For the growth of ZnO nanowires/nanosheets, a mixed aqueous solution of zinc nitrate hexahydrate [$Zn(NO_3)_2 \cdot 6H_2O$] (0.03 M), hexamethylenetetramine [$(CH_2)_6N_4$] (HMT) (0.03 M) and polyethylenimine (PEI) (0.003 M) was prepared. The patterned Al/ZnO seed substrates were dipped into this solution for 3 hours under stirring at 68 °C. The fabricated ZnO nanowire/nanosheet samples were then washed in de-ionized water and air-dried on a hot plate kept at 60 °C.

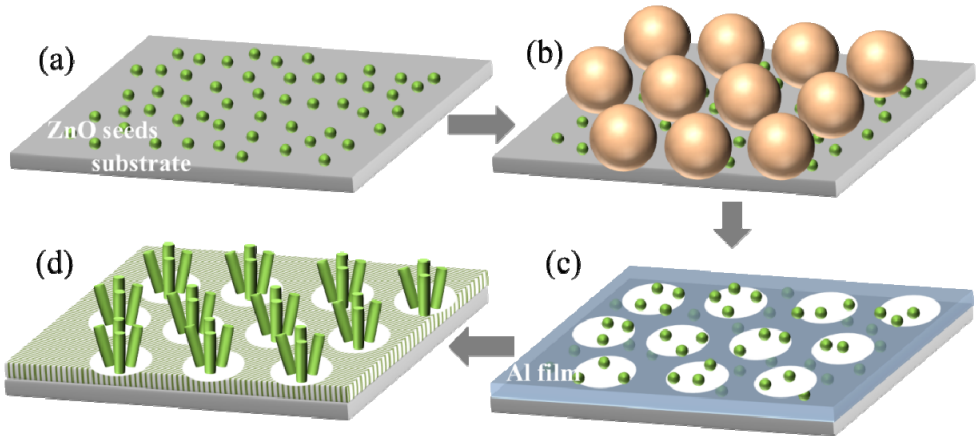

Fig. 1. Schematic of ZnO nanowire/nanosheet synthesis. (a) ZnO seeds were formed on the substrate. (b) A monolayer of PS sphere was deposited on top of the ZnO seeds. The size of the sphere can be adjusted with dry etching. (c) Al nanohole arrays were fabricated using the PS spheres as masks. (d) Patterned ZnO nanowires/nanosheets were grown from the same growth solution.

2.2 Characterization

Photoluminescence spectra of the samples were collected using a micro PL system (Horiba LabRam HR) with 325 nm He-Cd laser as the excitation source. SEM imaging and EDS were carried out inside a Hitachi FE-SEM (SU8000). High resolution TEM (HRTEM) imaging was done in a JEOL TEM (JEM 2100F) working at 200 kV.

3. Results and discussions

Figure 2 shows a typical SEM image of the boundary between the ZnO nanowire area and the nanosheet area. The nanowires are directly grown on cleaned ITO substrate with most of them pointing upward. The nanowires exhibit hexagonal cross-sections with the majority showing diameter in the range of 30-40 nm (Fig. 2, inset, bottom-left). By contrast, the ZnO nanostructures grown on Al thin film display sheet-like flat morphology. The nanosheets are either stacking together or intersecting with each other forming dense complex patterns and yielding high surface area. The thickness of the nanosheets is about 2-3 nm independent of their lateral dimensions.

Figure 3(a) shows the representative photoluminescence spectra of the synthesized nanowires and nanosheets from Fig. 2. The ZnO nanowires exhibit the band-edge emission at 382 nm together with a broad emission band centered around 600 nm, which is attributed to the oxygen defects in the ZnO nanowires as in earlier reports [27–29]. By contrast, the ZnO nanosheets show dramatically different PL spectra with a broad green band centered at 547 nm. Furthermore, no band-edge emission is observed from the nanosheets. Instead, a weak PL shoulder at 430 nm appears on the spectrum.

#226727 - $15.00 USD Received 12 Nov 2014; accepted 18 Dec 2014; published 13 Jan 2015

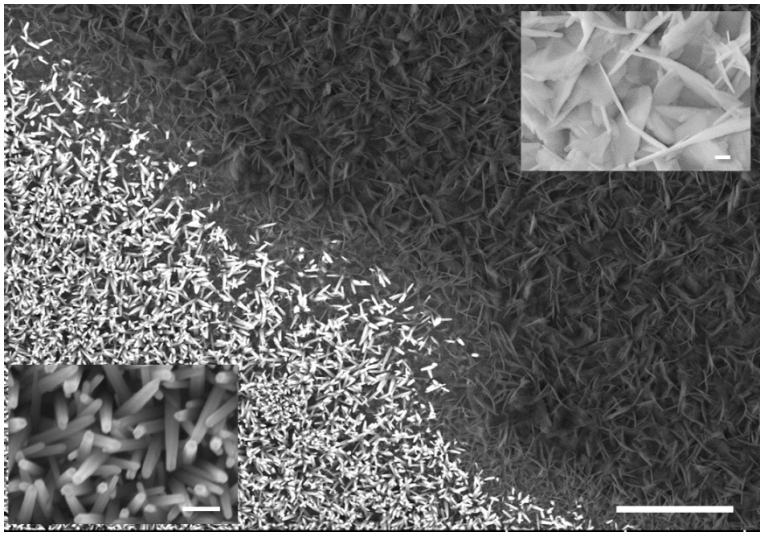

Fig. 2. SEM image of the boundary between the ZnO nanowire area (bottom-left) and nanosheet area (top-right). The scale bar is 5μm in length. Inset: magnified SEM images of nanowires (bottom-left) and nanosheets (top-right). The scale bar in either inset is 200 nm.

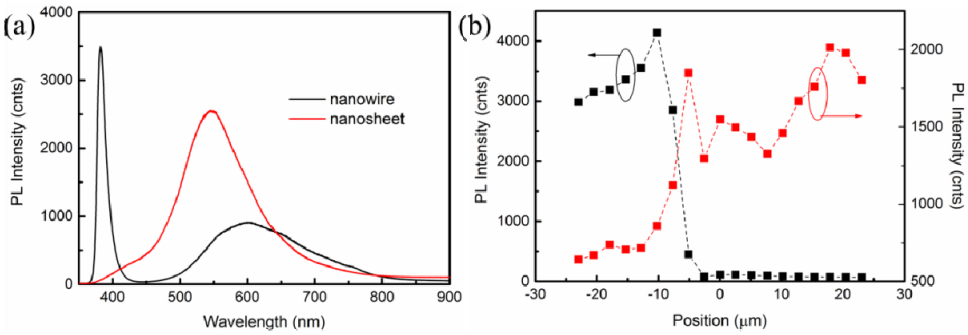

Fig. 3. (a) Representative PL spectra of ZnO nanowires (black) and nanosheets (red). Band-edge emission at 382 nm is only observed from the ZnO nanowires. (b) The variation of the PL intensity of the 382 nm peak (black, left axis) and 547 nm peak (red, right axis) along a line-scan across the nanowire/nanosheet boundary. The nanowires are located on the line below −7 μm while the nanosheets above −7 μm.

A PL line-scan was performed across the nanowire-nanosheet boundary. The 382 nm and 547 peak intensity were recorded and displayed in Fig. 3(b). It is clearly shown that the band-edge emission at 382 nm (black squares) experienced a sharp intensity drop, from 3000~4000 to 100, at the boundary (~-7 μm) when the excitation laser moved from the nanowire region to nanosheet region. By contrast, the intensity of the green emission at 547 nm (red squares) increases by 3-4 times concurrently. The changes of peak intensity show a good agreement with the spectra in Fig. 3(a). It is noted that, for the 547 nm peak intensity, there is a partial contribution from the 600 nm broad band in the nanowire region (< −7 μm), which results in the relatively smaller intensity contrast compared with 382 nm peak intensity (from ~3000 to ~100).

The distinctive photoluminescence properties of nanowires and nanosheets could be of great importance for a variety of applications. The above sample only displayed two regions with ZnO nanowires and nanosheets. Periodic patterns can be designed to create novel two-dimensional structures with highly tunable optical properties, which may find applications in light-emitting devices. Here, we employed another facile and widely-used technique -

#226727 - $15.00 USD Received 12 Nov 2014; accepted 18 Dec 2014; published 13 Jan 2015

colloidal lithography - to create periodic hexagonal pattern of the ZnO nanowires with nanosheets in between. In general, colloidal lithography produces monolayers of close-packed latex nanospheres/microspheres on substrates. With RIE, we can further reduce the size of the sphere while keep the periodicity intact.

Figure 4 shows the SEM images of the synthesized nanowire/nanosheet patterns. The dry etching time increases from panel *a* to *f* leading to decreased size of the Al nanoholes. In panels *a-c*, it can be seen that hexagonal patterns of the ZnO nanowire bunches are achieved with decreasing diameter of the bunch due to the shrinking Al nanoholes underneath while the periodicity is kept the same. Further reducing the size of the Al nanohole results in termination of the ZnO nanowire growth and the substrates were totally covered with ZnO nanosheets. However, it is clearly shown in the SEM images (*d-f*) that the morphology of the nanosheets inside the hole (on the ITO substrate) is different from those on the Al thin film. In general, the size of the former is smaller than that of the latter. In addition, more needle-like ZnO nanoobjects are accumulated in the hole region. Apparently, the Al film plays a critical role determining the morphologies of the grown ZnO nanostructures. It is reported that the formation of a boehmite layer is responsible for the growth of sheet-like ZnO nanostructures [15]. Thus, with this simple technique, not only are we able to create periodic ZnO nanowire patterns, but also we can control the morphology of the ZnO nanosheets and even realize periodic patterning of different ZnO nanosheets. Such a ZnO growth technique with high tunability could be applied to a wide range of applications for complex patterning and advanced optical property control.

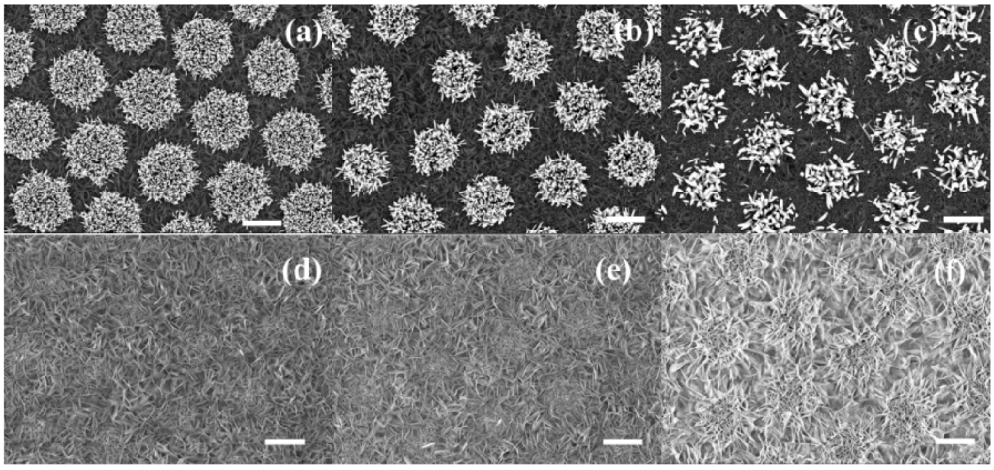

Fig. 4. SEM images of controllable periodic pattern of ZnO nanowires/nanosheets. The Al nanohole size is decreasing from panel a to panel f. For smaller hole size (panel d-f), ZnO nanowires are prevented from growing and ZnO nanosheets prevail. The scale bars in all panels are 2μm in length.

We investigated the PL properties of the periodic ZnO nanowire/nanosheet patterns. Figure 5 shows the optical image (Fig. 5(a), marked region) and the corresponding PL map (Fig. 5(b)). The darker circular areas in Fig. 5(a) are the ZnO nanowire bunches arranged in hexagonal pattern as in Fig. 4(b). We scanned the marked region and selected the band-edge emission 382 nm for PL mapping. As shown in Fig. 5(b), the large bright spots are the band-edge emissions from the bunched ZnO nanowires matching well with the optical image. Hence, a good correlation is achieved between the PL map and the marked optical image. The demonstrated technique here can provide simple and effective means to engineer the optical properties of the samples.

#226727 - $15.00 USD Received 12 Nov 2014; accepted 18 Dec 2014; published 13 Jan 2015

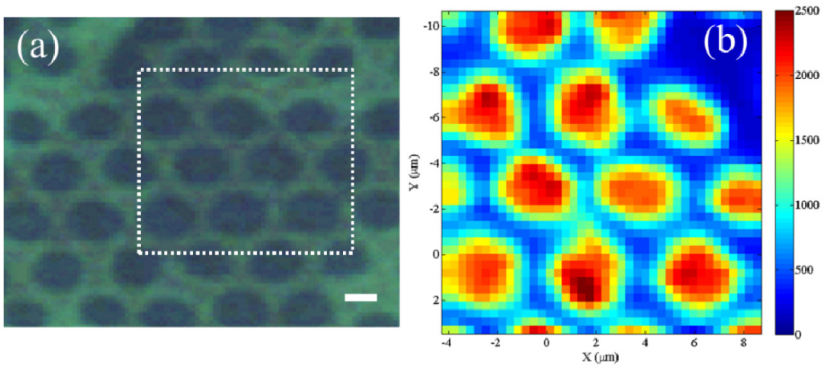

Fig. 5. (a) Optical image of ZnO nanowire/nanosheet substrate. (b) Corresponding PL mapping of the marked region in (a). The band-edge emission 382 nm is selected for imaging. The PL map shows good agreement with the optical image in the marked region. The scale bar in (a) is 2 μm.

Now we will try to explain the difference between the PL spectra of ZnO nanowires and nanosheets. It is known that various deep level native defects, such as oxygen and zinc vacancies, in ZnO nanostructures account for the broad visible PL bands observed from samples prepared with different techniques. However, the exact origins of these PL bands are still under debate [29–32]. It is believed that oxygen interstitials or the surface OH groups are responsible for the yellow-orange emission at 600 nm as we observed in the ZnO nanowires. For the most controversial green emission, latest study suggests that zinc vacancies are a more feasible source for the green PL band [30, 33]. This is qualitatively confirmed by mapping the distribution of element Zn and O on the sample by EDS as shown in Fig. 6. In Fig. 6(b), it is shown that there are more Zn elements in the nanowire regions than in the nanosheet regions. However, Fig. 6(c) reveals that more O elements exist in the ZnO nanosheet areas. Therefore, the O/Zn atom ratio is higher in the ZnO nanosheets than that in the ZnO nanowires. Closer examination reveals that the O/Zn atom ratio is about 2 in the ZnO nanosheet region indicating that Zn vacancies are abundant in the nanosheets giving rise to that strong green emission as observed in Fig. 3(a). The crystalline structures of the ZnO nanowire/nanosheet were further evaluated with high-resolution TEM as shown in Fig. 7. ZnO nanowire (Fig. 7(a)) shows single crystalline feature while nanosheet (Fig. 7(b)) exhibits polycrystalline nature, which makes it prone to defect growth and explains the absence of band edge emission at 382 nm.

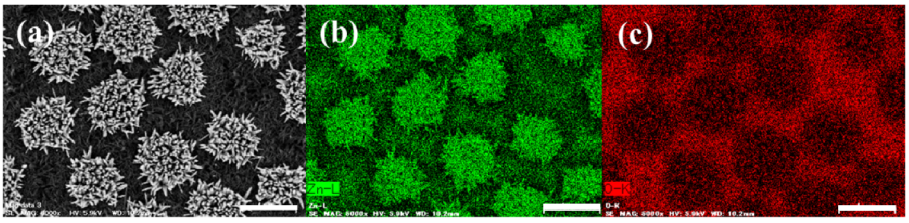

Fig. 6. SEM image of ZnO nanowire/nanosheet pattern (a) and the corresponding Zn (b) and O (c) distribution map obtained with EDS. The scale bars in all panels are 4 μm.

#226727 - $15.00 USD Received 12 Nov 2014; accepted 18 Dec 2014; published 13 Jan 2015

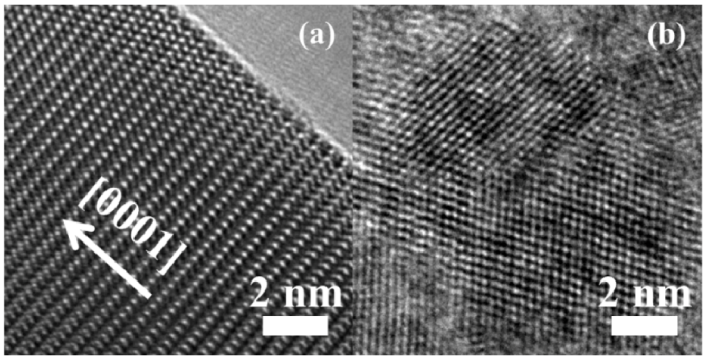

Fig. 7. High resolution TEM images of ZnO (a) nanowire and (b) nanosheet.

3. Conclusion

In conclusion, we have demonstrated well-controlled patterning of ZnO nanowires and nanosheets on ITO glass substrates modified with Al nanohole arrays, which were patterned by colloidal lithography. From the same growth solution, ZnO nanowires grow inside the Al nanohole (on the glass substrate) while ZnO nanosheets grow exclusively on the Al thin film. The size of the Al nanohole and thus the size of the nanowire bundle can be accurately controlled by etching time of the polystyrene spheres. The ZnO nanowires and nanosheets exhibit distinctive photoluminescence properties. The nanowires show the band-edge emission at 382 nm together with a broad yellow-orange band while the nanosheets only show a broad and strong green emission. This is attributed to the zinc vacancies in the nanosheets as confirmed by EDS mapping. The proposed fabrication technique here provides a facile means to control the optical properties of ZnO nanostructures over a large area, and can be of use for flexibly tailoring the active spectral region in ZnO-based light-emitting devices and for energy harvesting applications.

Acknowledgment

The authors would like to thank Prof. Masahiro Kitajima for helpful discussions.

#226727 - $15.00 USD Received 12 Nov 2014; accepted 18 Dec 2014; published 13 Jan 2015